Raman Spectroscopy

DOI: 10.1002/ange.200901807

Loading of Exponentially Grown LBL Films with Silver Nanoparticles and Their Application to Generalized SERS Detection**

Sara Abalde-Cela, Szushen Ho, Benito Rodríguez-González, Miguel A. Correa-Duarte, Ramón A. Álvarez-Puebla, Luis M. Liz-Marzán, and Nicholas A. Kotov**

Surface-enhanced Raman scattering (SERS)[1] is currently recognized as one of the most sensitive spectroscopic tools, which can be exploited for ultrasensitive chemical and biological detection[2] in addition to providing structural information[3] on the systems of interest. Since the study of the mechanisms behind the relationship between SERS and surface-plasmon-driven electromagnetic fields has progressed significantly,[4] research is turning toward the design of advanced materials capable of generating high-quality SERS signals from interesting analytes.[5] In this respect, several approaches have recently been reported that range from the coupling of highly aromatic molecules to nanostructured metallic surfaces that may attract nonpolar analytes of interest,[6] to the modification of surface charge to attract polar molecules that cannot be retained on gold or silver.[7] Unfortunately, only partial success has been achieved with these approaches because the coupled aromatic systems overlap and hide the signal from the analyte, whereas control of surface charge has only proven useful for the detection of carboxylic acids or amines, depending on the pH.

Recently, some of us successfully reported the use of thermoresponsive poly(*N*-isopropylacrylamide) (PNIPAM) microgels as molecular traps that can drive analytes toward Au nanoparticle (NP) cores.[8] Nevertheless, all of the previously mentioned techniques present some drawbacks, such as 1) the impossibility of forming hot spots, as the particles are completely isolated by a protective shell that inhibits their plasmonic interactions; 2) the use of gold limits the enhancing factor for SERS as compared with silver;[9] and 3) the presence of strongly damped plasmons in gold when excited with green or more energetic lasers because of coupling to interband transitions.[10] All these technological challenges require the development of a new type of SERS substrate, which would combine a high density of NPs inside a polymeric matrix, thus providing both access to hot spots and analyte retention. Thin films made by exponential layer-by-layer (e-LBL) growth do indeed display remarkably high diffusivity,[11] which in the past was predominantly used for drug-delivery applications. Interestingly, they can be readily infiltrated with inorganic NPs,[12,13] and have the ability to sequestrate molecular systems in solution as a function of the composition of their layers.

Herein, we demonstrate the infiltration of e-LBL films with silver NPs (AgNPs), as a means to generate a dense collection of three-dimensional hot spots that yield extraordinary SERS intensity over the whole surface in a wide spectral window, from the visible to the near infrared (NIR). Additionally, proof of concept of the sequestration of uncommon molecular systems is demonstrated through the first SERS analysis of dioxins, ubiquitous environmental pollutants generated as a by-product in the manufacture of organochlorides, incineration of chlorine-containing substances such as poly(vinyl chloride), paper bleaching, and from natural sources such as volcanoes, forest fires, and bacterial metabolism.[14] Rapid and sensitive identification of these substances is extremely important as they bioaccumulate in fatty tissues, so even small exposures may eventually reach dangerous levels.[15] These molecules have been classified as Group 1 carcinogens by the International Agency for Research on Cancer but are also responsible for several other pathologies, such as disorders of the central and peripheral nervous system and thyroid, damage to the immune system, or diabetes.[16]

The preparation of the matrix for the infiltration of AgNPs was carried out by exponential growth of LBL films of poly(diallyldimethylammonium chloride) (PDDA) and poly(acrylic acid) (PAA; see the Experimental Section for details). Prior to infiltration with AgNPs (diameter ≈ 5 nm),[17] films containing 30 PDDA–PAA bilayers, $(PDDA–PAA)_{30}$, were immersed in an aqueous sodium citrate (1%) solution for 12 h, during which the transparent films turned white. This pretreatment was essential for obtaining the correct organization of NPs within the film and to avoid rapid destabilization of NP dispersions. PDDA

[*] S. Abalde-Cela, Dr. B. Rodríguez-González, Dr. M. A. Correa-Duarte, Dr. R. A. Álvarez-Puebla, Prof. L. M. Liz-Marzán
Departamento de Química-Física and Unidad Asociada CSIC-Universidade de Vigo, 36310 Vigo (Spain)
E-mail: ramon.alvarez@uvigo.es
Homepage: http://webs.uvigo.es/coloides/nano
S. Ho, Prof. N. A. Kotov
Departments of Chemical Engineering, Materials Science and Engineering, and Biomedical Engineering, University of Michigan Ann Arbor, MI 48109 (USA)
E-mail: kotov@umich.edu
Homepage: http://www.engin.umich.edu/dept/che/research/kotov

[**] M.A.C.-D. acknowledges the Isidro Parga Pondal Program fellowship (Xunta de Galicia, Spain) and R.A.A.-P. acknowledges the Ramon y Cajal Program fellowship (Ministerio de Educacion y Ciencia, Spain). This work was funded by the Spanish Ministerio de Ciencia e Innovación (MAT2007-62696 and MAT2008-05755) and the Xunta de Galicia (PGIDIT06TMT31402PR and 08TMT008314PR). We thank A. Benedetti and C. Serra (CACTI, Universidade de Vigo) for carrying out the FIB sample preparation and XPS measurements, respectively. LBL = layer-by-layer; SERS = surface-enhanced Raman scattering.

Supporting information for this article is available on the WWW under http://dx.doi.org/10.1002/anie.200901807.

can freely diffuse inside PDDA–PAA e-LBL thin films. The outermost layer of the film is a thick layer of negatively charged PAA, which forms a barrier between negatively charged citrate-stabilized AgNPs and positively charged PDDA. Without the immersion in sodium citrate, PDDA can easily diffuse out from the thin film and cause the precipitation of the NP solution before infiltration of the NPs. With citrate pretreatment, PDDA is stabilized inside the film, thus leading to successful packing of NPs along PDDA chains.

The modified films were then immersed in an aqueous dispersion of AgNPs. Silver incorporation within the film was monitored by UV/Vis spectroscopy. Figure 1 shows the

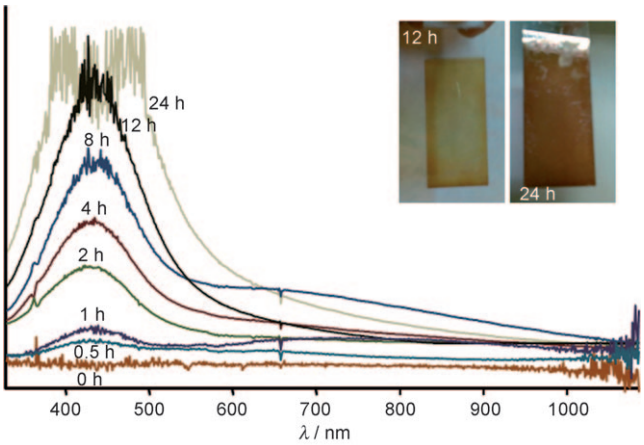

Figure 1. UV/Vis spectra of the e-LBL AgNP films as a function of the immersion time of the e-LBL film in a silver colloid. Inset: digital photographs of the films after 12 and 24 h of immersion.

increase in the intensity of the silver localized surface plasmon resonance (LSPR) band with time as more silver seeds are infiltrated. The LSPR, centered at 434 nm, continuously grows until saturation of the spectrometer detector. Notably, accumulation of the AgNPs inside the films was also visually evidenced by the color change of the films from white to dark yellow-orange after 24 h (see insets in Figure 1). Predominantly electrostatic interactions drive the NPs inside the films. After entering the matrix, however, they become entrapped by a variety of secondary interactions. Other films with a larger number of bilayers (54 and 100) were also successfully infiltrated with AgNPs, but the best results were consistently obtained with $(PDDA–PAA)_{30}$.

Scanning electron microscopy (SEM) imaging of the infiltrated films (Figure 2 A,B) shows that dendritic structures were formed by the infiltrated AgNPs. However, since SEM does not give a clear picture of the actual distribution of AgNPs within the film, cross-sectional imaging was carried out by cutting a thin lamella across the film using focused ion-beam (FIB) etching (see the Supporting Information for details and additional images). Figure 2 C and D show transmission electron microscopy (TEM) and scanning TEM (STEM) images, respectively, of the cross-sectional view of the lamella, and reveal a high density of AgNPs that penetrate 150 nm deep inside the polymer film. The particles range in size from 5 to 30 nm, which is in contrast to the initial size (5 nm) of the seeds used for the infiltration. This size increase

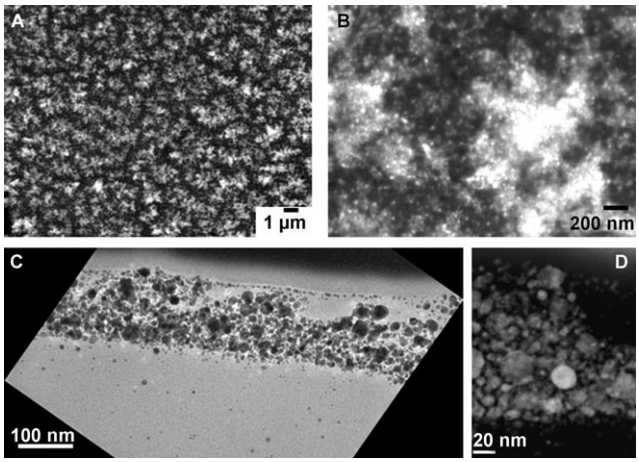

Figure 2. A,B) Top-view SEM images at different magnifications of the e-LBL AgNP film after 24 h of immersion. C,D) Cross-sectional TEM and STEM images, respectively, of the film after FIB preparation.

is ascribed to Ostwald ripening[18] and, together with the extensive aggregation within the films, is consistent with the plasmonic properties observed in Figure 1. Additionally, the increased particle diameter prevents the NPs from leaking out of the film, as has been observed with other small particles such as quantum dots.[13]

Chemical analysis of the films was carried out by X-ray photoelectron spectroscopy (XPS; Supporting Information, Figure S6). Remarkably, direct analysis of the films shows a spectrum mainly dominated by C 1s (285 eV) and O 1s (520 eV) with a smaller contribution by N 1s (402 eV), with weak intensity of the Ag $3d_{3/2}$ and $3d_{5/2}$ characteristic bands (374.2 and 368.3 eV), which indicates that the silver content at the surface is low. After etching the sample with an Ar^+ plasma, a substantially enhanced Ag signal was readily observed as a consequence of removal of the polymer,[19] which additionally demonstrates that AgNPs effectively infiltrate inside the polymer matrix. The three-dimensional aggregation of AgNPs may thus be considered to generate three-dimensional hot spots, which were expected to result in the generation of huge electromagnetic fields capable of enhancing the Raman signal accordingly.

To prove this last statement, samples were immersed in a 10^{-5} M solution of 1-naphthalenethiol (1NAT), a well-known Raman probe,[20] air dried, and the dry films were characterized with four different laser excitation lines ranging from the visible (532 and 633 nm) to the NIR (785 and 830 nm). In all cases, extremely strong SERS signals, around fivefold larger than those obtained from standard aggregated silver citrate colloids (Supporting Information, Figure S7), were acquired for the 1NAT characteristic bands (Figure 3 A): ring stretching (1553, 1503, and 1368 cm^{-1}), CH bending (1197 cm^{-1}), ring breathing (968 and 822 cm^{-1}), ring deformation (792, 664, 539, and 517 cm^{-1}), and CS stretching (389 cm^{-1}), even when using a very low laser power at the sample ($\approx$1 μW with acquisition times of 10 s). SERS mapping from the same region of the film surface was carried out by using all four laser lines (Figure 3 B). The results clearly indicate that the e-LBL NP films render an exceptionally efficient, portable SERS platform for a wide range of

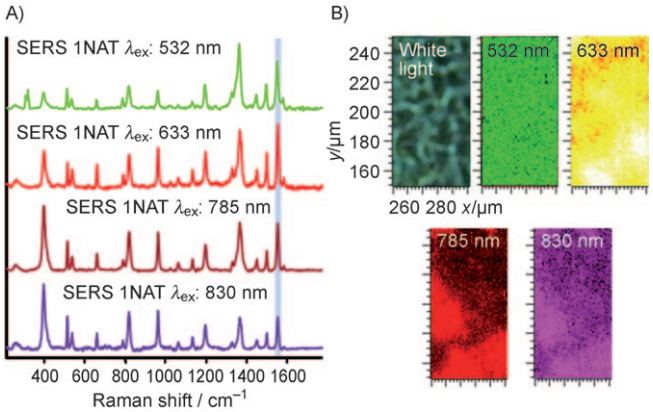

Figure 3. A) SERS spectra of 1NAT from a LBL Ag film using different excitation laser lines. B) SERS mapping of 1NAT (1553 cm^{-1}) on the films with different excitation laser lines (100×50 µm, step size 1 µm^2; 5000 spectra).

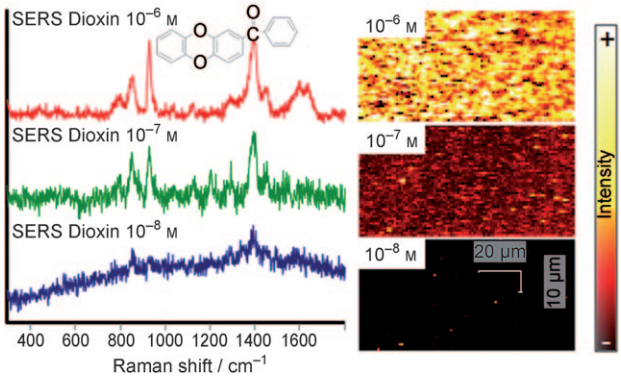

Figure 4. Left: SERS spectra of BDPD at different concentrations, from the e-LBL AgNP film, measured with a 633 nm laser line. Right: SERS mapping of the films (100×50 µm, step size 1 µm^2; 5000 spectra).

excitation laser lines with highly homogeneous signal intensity over the entire surface, which is often a critical parameter when dealing with hot spots built on solid thin films. Control experiments were carried out with the pure film, the film with 1NAT, and the film with NPs but no analyte, under the same conditions as in the SERS experiments. No significant vibrational pattern was observed in the spectra (Supporting Information, Figure S8), which confirms that the e-LBL AgNP films constitute excellent and clean platforms for SERS applications.

Analytical applications of the e-LBL AgNP substrates were tested toward the ultrasensitive analysis of a dioxin, 2-benzoyldibenzo-*p*-dioxin (BDPD). This analyte was chosen because, despite the interest in early and simple detection of minute amounts of this family of compounds, SERS analysis of dioxins remained elusive, as they do not stick to gold or silver surfaces. In this sense, and taking advantage of the molecular trapping properties of the e-LBL films, we designed a simple experiment. Briefly, e-LBL AgNP films were immersed for 2 h in aqueous solutions containing BDPD in concentrations ranging from 10^{-6} down to 10^{-9} M. Thereafter, the films were air dried and the surfaces were mapped by using a 633 nm laser line, which offers a good compromise between high SERS intensity and low sample damage.

Figure 4 shows the first ever reported SERS spectra for a dioxin, which are dominated by lines at 1392 (ring stretching) and 930 cm^{-1} (ring breathing), with a lower contribution of bands at 1641 (CO stretching), 1605 and 1445 (ring stretching), 1296 (CO stretching), 852 (CH wagging), and 791 cm^{-1} (ring deformation).[21] This vibrational pattern was reproducible through the entire surface (for the more concentrated sample) and between different samples. The SERS spectrum is still fully recognizable at concentrations down to 10^{-8} M, a level of detection that matches modern immunological methods[22] while avoiding sophisticated sample preparation.

In summary, we have devised and fabricated a universal SERS sensor based on e-LBL films infiltrated with AgNPs, which form three-dimensional hot spots. These films offer extremely high optical enhancement properties for a wide range of excitation energies, while maintaining the beneficial properties of e-LBL substrates related to molecular trapping and portability. Proof of concept for the analytical application of these materials was provided through the first SERS direct ultradetection of a dioxin. This new family of sensors paves the way for the simple, rapid, direct, and ultrasensitive SERS detection of pollutants that have been elusive so far, and other analytes of interest.

Experimental Section

Chemicals: All chemicals were purchased from Aldrich unless otherwise stated and used without further purification: PDDA (weight-average molecular weight, M_w: 10^5–2×10^5), PAA (M_w: 2.5×10^5), poly-4-styrene sulfonate (PSS, M_w: 1×10^6), silver nitrate, sodium borohydride, 1NAT (Acros Organics), and BDPD. Milli-Q water (Millipore) was used in all the experiments.

Polyelectrolyte multilayer buildup: Films of $(PDDA–PAA)_n$, where n is the number of bilayers (30, 54, and 100), were prepared by an automated dipping process (Stratosequence VI, Nanostrata) in PDDA (0.5% w/v in water, pH 6.8) and PAA (1.0% w/v in water, pH 2.9) solutions during 2 min. Each adsorption step was separated from the next one by two 1 min immersions in beakers containing pure water. The deposition of each PDDA and PAA "layer" defined one layer pair. The films were blown dry with an air flow after deposition of every layer pair.[13]

NP synthesis: AgNPs were produced by mixing aqueous solutions of trisodium citrate (25 mL, 25 mM), PSS (1.25 mL, 500 mg L^{-1}), and freshly prepared $NaBH_4$ (1.5 mL, 10 mM,) followed by addition of $AgNO_3$ (25 mL, 0.5 mM) at a rate of 2 mL min^{-1} with continuous stirring.[5] The final suspension was bright yellow.[23]

NP infiltration into $(PDDA–PAA)_n$ films: The $(PDDA–PAA)_n$ films used for silver infiltration were immersed in trisodium citrate solution (30 mL, 40 mM) for 24 h. Then the films were dipped in Milli-Q water and incubated inside the silver seed suspension for 24 h. The films were dipped in water after 0.5, 1, 2, 4, 8, and 12 h and immersed again in the NP suspension.

Characterization: Optical characterization was carried out by UV/Vis/NIR spectroscopy with a Cary 5000 spectrophotometer. SEM images were obtained with a JEOL JSM 6700F field-emission microscope. A dedicated backscattered electron detector (Autrata YAG detector) was used to enhance the signal from silver particles. The specimen for TEM was prepared by the lift-out technique in a FIB workstation with a FEI Helios 400 NanoLab dual-beam microscope. The final thickness of the lamella was about 50 nm. To protect the delicate surface features of the sample, it was coated with a thin layer of carbon prior to Pt coating and thinning. The lamella was then

transferred to a JEOL JEM 2010F transmission electron microscope for analysis. TEM images were acquired at 200 kV in bright field, whereas STEM images were obtained in a dark field mode.

XPS analysis of the samples was performed with a VG Escalab 250 iXL ESCA instrument (VG Scientific), equipped with $Al_{K\alpha}$ 1.2 monochromatic radiation at a 1486.92 eV X-ray source.

SERS measurements: SERS experiments were conducted with a micro-Raman Renishaw InVia Reflex system. The spectrograph used high-resolution gratings (1200 or 1800 $g\,mm^{-1}$) with additional bandpass-filter optics. Several laser excitation energies were employed, including laser lines at 532 (Nd:YAG), 633 (HeNe), and 785 and 830 nm (diode). All measurements were made in a confocal microscope in backscattering geometry using a 50× objective with a numerical aperture (NA) value of 0.75, which provided scattering areas of $\approx 1\ \mu m^2$. For SERS measurements, films were immersed in 1NAT or BDPD solutions of varying concentrations and air dried. The power at the sample was maintained as low as $\approx 1\ \mu W$. Acquisition times for spectra collection in extended mode, using the Renishaw continuous grating mode, were 10 s. SERS maps were collected by using the Renishaw StreamLine accessory with a step size of 1 μm.

Received: April 3, 2009
Revised: April 26, 2009
Published online: June 12, 2009

Keywords: layer-by-layer technique · nanoparticles · Raman spectroscopy · thin films · trace analysis

[1] a) P. L. Stiles, J. A. Dieringer, N. C. Shah, R. R. Van Duyne, *Annu. Rev. Anal. Chem.* **2008**, *1*, 601; b) K. Kneipp, *Phys. Today* **2007**, *60*, 40.

[2] a) M. Sanles-Sobrido, W. Exner, L. Rodriguez-Lorenzo, B. Rodriguez-Gonzalez, M. A. Correa-Duarte, R. A. Alvarez-Puebla, L. M. Liz-Marzan, *J. Am. Chem. Soc.* **2009**, *131*, 2699; b) K. Hering, D. Cialla, K. Ackermann, T. Dörfer, R. Möller, H. Schneidewind, R. Mattheis, W. Fritzsche, P. Rösch, J. Popp, *Anal. Bioanal. Chem.* **2008**, *390*, 113; c) C. Schmuck, P. Wich, B. Küstner, W. Kiefer, S. Schlücker, *Angew. Chem.* **2007**, *119*, 4870; *Angew. Chem. Int. Ed.* **2007**, *46*, 4786; d) G. Braun, S. J. Lee, M. Dante, T.-Q. Nguyen, M. Moskovits, N. Reich, *J. Am. Chem. Soc.* **2007**, *129*, 6378; e) J. Kneipp, H. Kneipp, K. Kneipp, *Chem. Soc. Rev.* **2008**, *37*, 1052.

[3] a) T. Hasegawa, *Biopolymers* **2004**, *73*, 457; b) R. A. Alvarez-Puebla, J. J. Garrido, R. F. Aroca, *Anal. Chem.* **2004**, *76*, 7118.

[4] a) E. C. Le Ru, E. Blackie, M. Meyer, P. G. Etchegoin, *J. Phys. Chem. C* **2007**, *111*, 13794; b) J. P. Camden, J. A. Dieringer, Y. Wang, D. J. Masiello, L. D. Marks, G. C. Schatz, R. P. Van Duyne, *J. Am. Chem. Soc.* **2008**, *130*, 12616; c) J. Zhao, A. O. Pinchuk, J. M. McMahon, S. Z. Li, L. K. Alisman, A. L. Atkinson, G. C. Schatz, *Acc. Chem. Res.* **2008**, *41*, 1710; d) S. J. Lee, Z. Q. Guan, H. X. Xu, M. Moskovits, *J. Phys. Chem. C* **2007**, *111*, 17985.

[5] a) T. A. Laurence, G. Braun, C. Talley, A. Schwartzberg, M. Moskovits, N. Reich, T. Huser, *J. Am. Chem. Soc.* **2009**, *131*, 162; b) H. Ko, S. Singamaneni, V. V. Tsukruk, *Small* **2008**, *4*, 1576; c) R. A. Tripp, R. A. Dluhy, Y. Zhao, *Nano Today* **2008**, *3*, 31; d) L. Brus, *Acc. Chem. Res.* **2008**, *41*, 1742; e) J. P. Camden, J. A. Dieringer, J. Zhao, R. P. Van Duyne, *Acc. Chem. Res.* **2008**, *41*, 1653; f) R. Gordon, D. Sinton, K. L. Kavanagh, A. G. Brolo, *Acc. Chem. Res.* **2008**, *41*, 1049; g) B. D. Piorek, S. J. Lee, J. G. Santiago, M. Moskovits, S. Banerjee, C. D. Meinhart, *Proc. Natl. Acad. Sci. USA* **2007**, *104*, 18898; h) L. Rodriguez-Lorenzo, R. A. Alvarez-Puebla, I. Pastoriza-Santos, S. Mazzucco, O. Stephan, M. Kociak, L. M. Liz-Marzan, F. J. Garcia de Abajo, *J. Am. Chem. Soc.* **2009**, *131*, 4616; i) M. Spuch-Calvar, L. Rodriguez-Lorenzo, M. P. Morales, R. A. Alvarez-Puebla, L. M. Liz-Marzan, *J. Phys. Chem. C* **2009**, *113*, 3373.

[6] a) L. Guerrini, J. V. Garcia-Ramos, C. Domingo, S. Sanchez-Cortes, *Anal. Chem.* **2009**, *81*, 953; b) L. Guerrini, J. V. Garcia-Ramos, C. Domingo, S. Sanchez-Cortes, *Anal. Chem.* **2009**, *81*, 1418; c) L. Guerrini, J. V. Garcia-Ramos, C. Domingo, S. Sanchez-Cortes, *Langmuir* **2006**, *22*, 10924.

[7] a) R. A. Alvarez-Puebla, R. F. Aroca, *Anal. Chem.* **2009**, *81*, 2280; b) S. Tan, M. Erol, S. Sukhishvili, H. Du, *Langmuir* **2008**, *24*, 4765; c) R. A. Alvarez-Puebla, E. Arceo, P. J. G. Goulet, J. J. Garrido, R. F. Aroca, *J. Phys. Chem. B* **2005**, *109*, 3787.

[8] R. A. Álvarez-Puebla, R. Contreras-Caceres, I. Pastoriza-Santos, J. Perez-Juste, L. M. Liz-Marzan, *Angew. Chem.* **2009**, *121*, 144; *Angew. Chem. Int. Ed.* **2009**, *48*, 138.

[9] J. Zhao, A. O. Pinchuk, J. M. McMahon, S. Li, L. K. Ausman, A. L. Atkinson, G. C. Schatz, *Acc. Chem. Res.* **2008**, *41*, 1710.

[10] a) M. Moskovits, *Rev. Mod. Phys.* **1985**, *57*, 783–826; b) D.-Y. Wu, X.-M. Liu, S. Duan, X. Xu, B. Ren, S.-H. Lin, Z.-Q. Tian, *J. Phys. Chem. C* **2008**, *112*, 4195; c) M. Rycenga, K. K. Hou, C. M. Cobley, A. G. Schwartz, P. H. C. Camargo, Y. Xia, *Phys. Chem. Chem. Phys.* **2009**, DOI: 10.1039/b903533h; d) C. M. Aikens, G. C. Schatz, *J. Phys. Chem. A* **2006**, *110*, 13317–13324; e) P. G. Etchegoin, E. C. Le Ru, M. Meyer, *J. Chem. Phys.* **2006**, *125*, 164705.

[11] a) G. Decher, *Science* **1997**, *277*, 1232; b) C. Picart, P. Lavalle, P. Hubert, F. J. G. Cuisinier, G. Decher, P. Schaaf, J.-C. Voegel, *Langmuir* **2001**, *17*, 7414; c) E. Hübsch, G. Fleith, J. Fatisson, P. Labbe, J. C. Voegel, P. Schaaf, V. Ball, *Langmuir* **2005**, *21*, 3664.

[12] P. Podsiadlo, M. Michel, J. Lee, E. Verploegen, N. Wong Shi Kam, V. Ball, J. Lee, Y. Qi, A. J. Hart, P. T. Hammond, N. A. Kotov, *Nano Lett.* **2008**, *8*, 1762.

[13] S. Srivastava, V. Ball, P. Podsiadlo, J. Lee, P. Ho, N. A. Kotov, *J. Am. Chem. Soc.* **2008**, *130*, 3748.

[14] a) M. Bunge, L. Adrian, A. Kraus, M. Opel, W. G. Lorenz, J. R. Andreesen, H. Görisch, U. Lechner, *Nature* **2003**, *421*, 357; b) J. I. Baker, R. A. Hites, *Environ. Sci. Technol.* **2000**, *34*, 2879.

[15] a) S. M. Hays, L. L. Aylward, *Regul. Toxicol. Pharmacol.* **2003**, *37*, 202; b) M. Van Den Berg, J. De Jongh, H. Poiger, J. R. Olson, *Crit. Rev. Toxicol.* **1994**, *24*, 1.

[16] a) P. A. Bertazzi, D. Consonni, S. Bachetti, M. Rubagotti, A. Baccarelli, C. Zocchetti, A. C. Pesatori, *Am. J. Epidemiol.* **2001**, *153*, 1031; b) M. Kogevinas, H. Becher, T. Benn, P. A. Bertazzi, P. Boffetta, H. B. Bueno-de-Mesquita, D. Coggon, D. Colin, D. Flesch-Janys, M. Fingerhut, L. Green, T. Kauppinen, M. Littorin, E. Lynge, J. D. Mathews, M. Neuberger, N. Pearce, R. Saracci, *Am. J. Epidemiol.* **1997**, *145*, 1061; c) J. P. Whitlock, Jr., *Chem. Res. Toxicol.* **1993**, *6*, 754.

[17] V. Bastys, I. Pastoriza-Santos, B. Rodríguez-González, R. Vaisnoras, L. M. Liz-Marzán, *Adv. Funct. Mater.* **2006**, *16*, 766.

[18] a) X. Wu, P. L. Redmond, H. Liu, Y. Chen, M. Steigerwald, L. Brus, *J. Am. Chem. Soc.* **2008**, *130*, 9500; b) C. Xue, G. S. Meitraux, J. E. Millstone, C. A. Mirkin, *J. Am. Chem. Soc.* **2008**, *130*, 8337.

[19] J. Zhang, Y. Gao, R. A. Alvarez-Puebla, J. M. Buriak, H. Fenniri, *Adv. Mater.* **2006**, *18*, 3233.

[20] R. A. Alvarez-Puebla, D. S. Dos Santos, Jr., R. F. Aroca, *Analyst* **2004**, *129*, 1251.

[21] T. Fujii, K. Tanaka, H. Tokiwa, Y. Soma, *J. Phys. Chem.* **1996**, *100*, 4810.

[22] Y. Inuyama, C. Nakamura, T. Oka, Y. Yoneda, I. Obataya, N. Santo, J. Miyake, *Biosens. Bioelectron.* **2007**, *22*, 2093.

[23] D. Aherne, D. M. Ledwith, M. Gara, J. M. Kelly, *Adv. Funct. Mater.* **2008**, *18*, 2005.

